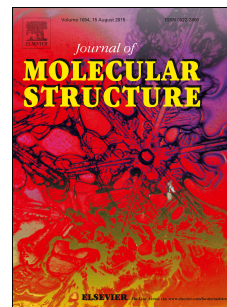


Journal Pre-proof

Synthesis, characterization, crystal structure and evaluation of four carbazole-coumarin hybrids as multifunctional agents for the treatment of Alzheimer's disease

Da-Hua Shi, Wei Min, Meng-qiu Song, Xin-Xin Si, Ming-Cheng Li, Zhao-yuan Zhang, Yu-Wei Liu, Wei-Wei Liu



PII: S0022-2860(20)30221-0

DOI: <https://doi.org/10.1016/j.molstruc.2020.127897>

Reference: MOLSTR 127897

To appear in: *Journal of Molecular Structure*

Received Date: 15 October 2019

Revised Date: 1 February 2020

Accepted Date: 12 February 2020

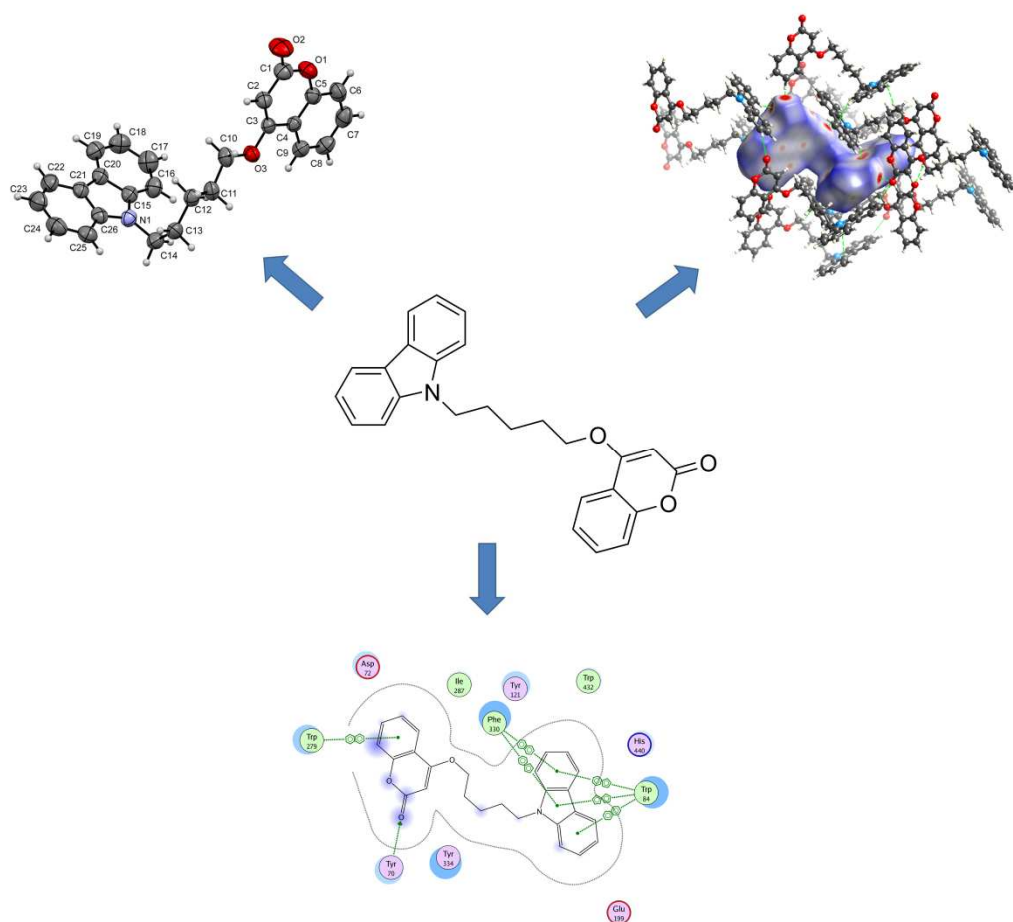
Please cite this article as: D.-H. Shi, W. Min, M.-q. Song, X.-X. Si, M.-C. Li, Z.-y. Zhang, Y.-W. Liu, W.-W. Liu, Synthesis, characterization, crystal structure and evaluation of four carbazole-coumarin hybrids as multifunctional agents for the treatment of Alzheimer's disease, *Journal of Molecular Structure* (2020), doi: <https://doi.org/10.1016/j.molstruc.2020.127897>.

This is a PDF file of an article that has undergone enhancements after acceptance, such as the addition of a cover page and metadata, and formatting for readability, but it is not yet the definitive version of record. This version will undergo additional copyediting, typesetting and review before it is published in its final form, but we are providing this version to give early visibility of the article. Please note that, during the production process, errors may be discovered which could affect the content, and all legal disclaimers that apply to the journal pertain.

© 2020 Published by Elsevier B.V.

Credit author statement

Da-Hua Shi: Conceptualization, Methodology, Software. **Wei Min:** synthesis, Writing- Original draft preparation. **Meng-qiu Song:** ChE-inhibition activity. **Xin-Xin Si:** ChE-inhibition activity. **Ming-Cheng Li:** antioxidant activity. **Zhao-yuan Zhang:** synthesis. **Yu-Wei Liu:** Molecular modeling study. **Wei-Wei Liu:** X-ray diffraction analysis.



Synthesis, characterization, crystal structure and evaluation of four carbazole-coumarin hybrids as multifunctional agents for the treatment of Alzheimer's disease

Da-Hua Shi^{a,b,*}, Wei Min^a, Meng-qiu Song^a, Xin-Xin Si^a, Ming-Cheng Li^a, Zhao-yuan Zhang^a, Yu-Wei Liu^a and Wei-Wei Liu^a

^a School of Pharmacy, Jiangsu Ocean University, Lianyungang 222005, People's Republic of China

^b Co-Innovation Center of Jiangsu Marine Bio-industry Technology, Lianyungang 222005, People's Republic of China

Abstract

Coupling of two distinct pharmacophores, carbazole and coumarin, endowed with different biological properties, afforded four hybrid compounds. The structures of the carbazole-coumarin hybrids were characterized by FT-IR, NMR, HRMS and single-crystal X-ray diffraction studies. All of these compounds exhibited significant acetylcholinesterase inhibitory activities. Among them, compound 4-((5-(9H-carbazol-9-yl)pentyl)oxy)-2H-chromen-2-one (**3d**) exhibited the best inhibition activity with IC₅₀ of 3.75 μM for acetylcholinesterase from *electric eel* and 70.51 μM for human recombinant acetylcholinesterase. Moreover, the compound 7-(3-(9H-carbazol-9-yl)propoxy)-4-methyl-2H-chromen-2-one (**3a**) had the best antioxidant activity. The docking studies demonstrated that compound **3d** could interact with both the catalytic active site and the peripheral anionic site of acetylcholinesterase. These attributes imply carbazole-coumarin hybrids as multifunctional agents for the Alzheimer's disease treatment.

Keywords: carbazole-coumarin hybrids, acetylcholinesterase, antioxidant, Alzheimer's disease

* Correspondent. E-Mail: shidahua@jou.edu.cn

1. Introduction

Alzheimer's disease (AD, MIM No. 104300) is an irreversible brain-producing disorder and the most common type of dementia (60-80%)[1]. Although the exact cause of AD remains unknown, several factors including low levels of neurotransmitter acetylcholine (ACh), the aggregation of β -amyloid ($A\beta$) peptide, dyshomeostasis of biometals, hyperphosphorylation of tau protein, and oxidative stress, are suggested to play important roles in the pathogenesis of AD[2, 3]. The numerous results achieved for AD treatment, but few goes to clinic trials or offers satisfied outcomes.

Cholinesterase inhibitors (ChEIs) are the well-studied compounds for the treatment of AD based on the cholinergic hypothesis. These drug candidates are prior options for patients with mild to moderate AD, and can alleviate symptom of cognitive dysfunction[4, 5]. The main function of Cholinesterases (ChE) including acetylcholinesterase (AChE) and butyrylcholinesterase (BuChE), is to hydrolyze cholinergic neurotransmitters[6]. AChE can also induce $A\beta$ aggregation (another marker of AD) through direct interaction of its PAS with $A\beta$ peptide. According to X-ray structural analysis, there is a narrow and deep canyon in the active site of AChE. Two different binding sites are included: the catalytic active site (CAS) at the bottom of the canyon and the peripheral anion binding site (PAS) at the entrance to the canyon[7]. Accordingly, AChE inhibitors can be categorized as single- and two-site inhibitors[7, 8]. It is believed that AChE inhibitors interacting with both CAS and PAS appear to be more beneficial for AD treatment[8, 9].

Antioxidants have drawn much attention recently in AD treatment. Increases of damaged macromolecules such as nucleic acids, proteins, lipids have been observed in AD brains. These findings support reactive oxygen species (ROS) plays a pivotal role in the pathogenesis of AD[10]. Therefore, antioxidants should have great benefits in the treatment of AD[11].

Due to the complex nature of AD, most of the single-target directed drug candidates failed to reach clinical trials. Thus, multi-target-directed ligands (MTDLs) are considered as an effective alternative for the treatment of AD[12, 13]. Various

coumarin-based hybrids possessing diverse medicinal attributes were synthesized[14]. Studies have also shown that both naturally occurring and synthetic coumarin analogues exhibit potent AChE, BuChE, dual AChE/BuChE and monoamine oxidase (MAO) inhibitory activity[15-17]. More and more coumarin core contained MTDLs with AChE inhibitory activity have been designed and synthesized [2, 18-22]. Carbazoles are naturally occurring phytochemicals in many plants with a wide range of biological activities. Some carbazole derivatives possessed AD-related biological activities[23]. It is reported that naturally occurring carbazole derivatives have strong antioxidant capacity and can directly scavenge ROS[24]. In addition, studies have shown that carbazole derivatives can inhibit $A\beta$ aggregation[25]. It is reported that carbazole derivatives which could be regarded as the D-ring opened analogs of galantamine could inhibit ChE and protect neurons from the toxicity induced by β -amyloid[26]. Many carbazole derivatives were designed as MTDLs for the treatment of AD[27-29]. In the present study, we synthesized and evaluated four carbazole-coumarin hybrids as MTDLs for the treatment of AD.

2. Experimental

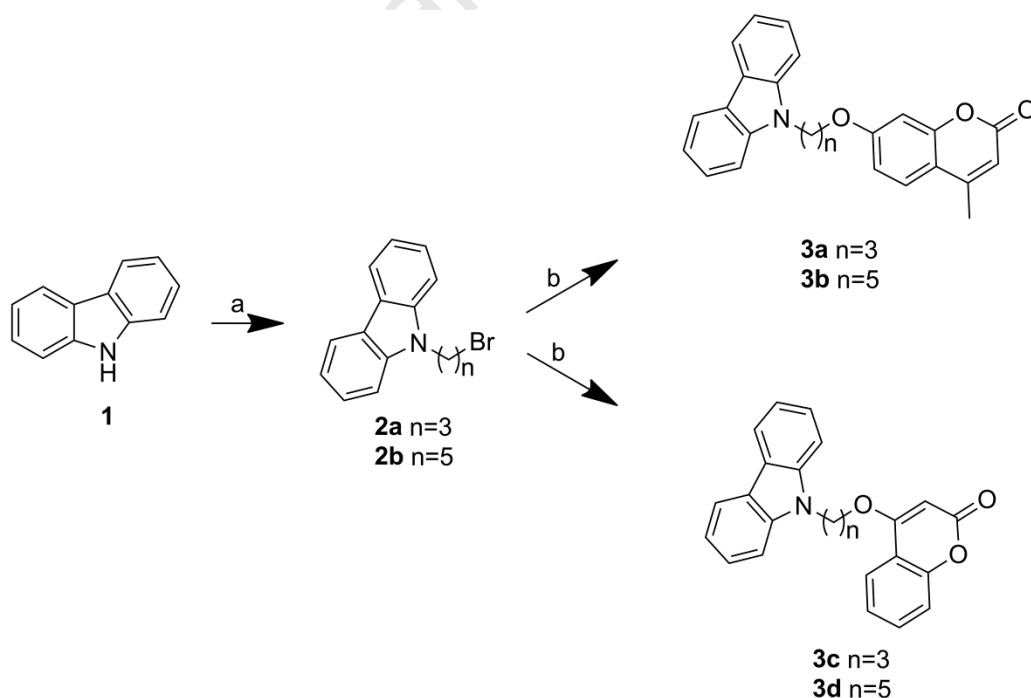
2.1. General instrumentations and materials

All synthetic reagents with AR grade were purchased from Aladdin Industrial Corporation and were used as received. AChE from *electric eel* (*eeAChE*) and human recombinant AChE (*hAChE*), BuChE from equine serum (*eqBuChE*) and human serum (*hBuChE*) were purchased from Sigma-Aldrich. TLC was performed on the glassbacked silica gel sheets (Silica Gel 60 GF254) and visualized in UV light (254 nm). All the melting points were determined by Kohler melting point apparatus. The NMR spectra were recorded in $CDCl_3$ solvent on a Bruker Avance 600 MHz instrument. Infrared (IR) spectra were recorded on a Thermo Scientific Nicolet iS10 spectrometer in KBr. High resolution mass spectra (HRMS) were recorded using HPLC 1260-6230 TOF MASS. The X-ray single crystal diffraction data were recorded on a Bruker SMART APEX-II CCD diffractometer.

2.2. General procedure for the synthesis of compounds **3a** – **3d**

The synthetic routes to final compounds **3a** – **3d** were depicted in **Schemes 1**. A

mixture of carbazole (1.79 mmol), α,ω - dibromoalkane (7.2 mmol), tetrabutylammonium bromide (TBAB) (1.79 mmol) were combined in benzene (4 mL) and NaOH solution (0.5 M, 4 mL). The reaction mixture was stirred at 55 °C for 6 h. After cooling, ethyl acetate (20 mL) was added to the solution, then the solution washed with saturated sodium chloride (20 mL) solution three times. The ethyl acetate phase was dried over anhydrous sodium sulfate and evaporated under reduced pressure to yield the crude product that was purified by column chromatography using petroleum ether and ethyl acetate (4:1) as an eluent to obtain **2a** and **2b**. A mixture of **2a** or **2b** (1.2 mmol), K_2CO_3 (0.6 mmol), coumarin (3.6 mmol) were combined in DMF (4 mL). The mixture was stirred at 55 °C for 3 h and ethyl acetate (20 mL) was added to the solution, then the solution washed with saturated sodium chloride (20 mL) solution three times. The ethyl acetate phase was dried over anhydrous sodium sulfate and evaporated under reduced pressure to yield the crude product that was purified by column chromatography using petroleum ether and ethyl acetate (2:1) as an eluent to obtain compound **3a – 3d**.



Schemes 1. Synthesis of final compounds **3a – 3d**. Reagents and conditions: (a) α,ω - dibromoalkane, TBAB, NaOH, benzene, 55°C, 6h; (b) coumarin, anhydrous K_2CO_3 , DMF, 55°C, 3h.

2.2.1. 9-(3-bromopropyl)-9H-carbazole (**2a**)

White solid; yield 56%; mp 40 – 42 °C; IR (KBr): 3425, 3046, 2963, 2359, 2358, 2339, 1928, 1891, 1769, 1626 cm⁻¹. ¹H NMR (500 MHz, Chloroform-*d*) δ 8.10 (d, *J* = 7.8 Hz, 2H), 7.51 – 7.44 (m, 4H), 7.25 – 7.21 (m, 2H), 4.49 (t, *J* = 6.5 Hz, 2H), 3.37 (t, *J* = 6.2 Hz, 2H), 2.42 (p, *J* = 6.4 Hz, 2H). ¹³C NMR (126 MHz, Chloroform-*d*) δ 140.3, 125.8, 122.9, 120.4, 119.1, 108.6, 40.9, 31.9, 30.9.

2.2.2. 9-(5-bromopentyl)-9H-carbazole (**2b**)

White solid; yield 60%; mp 53 – 55 °C; IR (KBr): 3440, 3047, 2924, 2859, 2359, 2340, 1936, 1898, 1782, 1625 cm⁻¹. ¹H NMR (500 MHz, Chloroform-*d*) δ 8.09 (d, *J* = 7.7 Hz, 2H), 7.45 (t, *J* = 7.6 Hz, 2H), 7.37 (d, *J* = 8.2 Hz, 2H), 7.22 (t, *J* = 7.4 Hz, 2H), 4.28 (t, *J* = 7.2 Hz, 2H), 3.32 (t, *J* = 6.7 Hz, 2H), 1.85 (dp, *J* = 14.3, 7.1 Hz, 4H), 1.53 – 1.46 (m, 2H). ¹³C NMR (126 MHz, Chloroform-*d*) δ 140.3, 125.7, 122.8, 120.4, 118.8, 108.6, 42.8, 33.3, 32.5, 28.2, 25.9.

2.2.3. 7-(3-(9H-carbazol-9-yl)propoxy)-4-methyl-2H-chromen-2-one (**3a**)

White powder; yield 64%; mp 197 – 199 °C; IR (KBr): 3059, 2931, 2877, 2360, 2341, 1706, 1610 cm⁻¹. ¹H NMR (600 MHz, Chloroform-*d*) δ 8.10 (d, *J* = 7.8 Hz, 2H), 7.48 (d, *J* = 8.9 Hz, 1H), 7.42 – 7.37 (m, 4H), 7.22 (ddd, *J* = 7.9, 6.0, 2.1 Hz, 2H), 6.83 (dd, *J* = 8.8, 2.4 Hz, 1H), 6.74 (d, *J* = 2.4 Hz, 1H), 6.16 – 6.12 (d, *J* = 1.1 Hz, 1H), 4.57 (t, *J* = 6.5 Hz, 2H), 3.93 (t, *J* = 5.6 Hz, 2H), 2.40 (m, 5H). ¹³C NMR (151 MHz, Chloroform-*d*) δ 161.6, 161.3, 155.2, 152.5, 140.4, 125.8, 125.6, 122.9, 120.4, 119.1, 113.8, 112.3, 112.1, 108.4, 101.6, 65.1, 39.2, 28.5, 18.7. HRMS: (ESI, *m/z*): [M+Na]⁺ calcd for C₂₅H₂₁NO₃ 406.1414, found 406.1429.

2.2.4. 7-(5-(9H-carbazol-9-yl)butoxy)-4-methyl-2H-chromen-2-one (**3b**)

White solid; yield 61%; mp 150 – 152 °C; IR (KBr): 3094, 2942, 2867, 2358, 2337, 1704, 1608 cm⁻¹. ¹H NMR (600 MHz, Chloroform-*d*) δ 8.10 (d, *J* = 7.7 Hz, 2H), 7.48 – 7.43 (m, 3H), 7.41 (d, *J* = 8.2 Hz, 2H), 7.23 (ddd, *J* = 7.9, 7.0, 0.9 Hz, 2H), 6.77 (dd, *J* = 8.8, 2.5 Hz, 1H), 6.74 (d, *J* = 2.5 Hz, 1H), 6.12 – 6.11 (d, *J* = 1.2 Hz, 1H), 4.34 (t, *J* = 7.1 Hz, 2H), 3.94 (t, *J* = 6.3 Hz, 2H), 2.37 (d, *J* = 1.2 Hz, 3H), 1.98 – 1.93 (m, 2H), 1.85 – 1.81 (m, 2H), 1.56 (m, 2H). ¹³C NMR (151 MHz, Chloroform-*d*) δ 161.9, 161.3, 155.1, 152.5, 140.3, 125.6, 125.4, 122.8, 120.3, 118.7, 113.4, 112.4,

111.8, 108.5, 101.3, 68.1, 42.8, 28.8, 28.7, 23.7, 18.6. HRMS: (ESI, m/z): [M+Na]⁺ calcd for C₂₇H₂₅NO₃ 434.1727, found 434.1741.

2.2.5. 4-(3-(9H-carbazol-9-yl)propoxy)-2H-chromen-2-one (**3c**)

White solid; yield 52%; mp 200 – 202 °C; IR (KBr): 3068, 2933, 2882, 2360, 2337, 1705, 1626 cm⁻¹. ¹H NMR (600 MHz, CDCl₃) δ 8.08 (d, *J* = 7.7 Hz, 2H), 7.77 (dd, *J* = 7.9, 1.6 Hz, 1H), 7.58 (ddd, *J* = 8.6, 7.2, 1.6 Hz, 1H), 7.42 – 7.28 (m, 6H), 7.22 (ddd, *J* = 7.9, 6.6, 1.5 Hz, 2H), 5.46 (s, 1H), 4.59 (t, *J* = 6.5 Hz, 2H), 4.02 (t, *J* = 5.7 Hz, 2H), 2.49 (p, *J* = 6.1 Hz, 2H). ¹³C NMR (151 MHz, Chloroform-*d*) δ 165.1, 162.7, 153.3, 140.2, 132.5, 125.9, 124.0, 123.0, 122.7, 120.6, 119.3, 116.9, 115.5, 108.2, 90.8, 66.3, 39.3, 28.0. HRMS: (ESI, m/z): [M+Na]⁺ calcd for C₂₄H₁₉NO₃ 392.1257, found 392.1262.

2.2.6. 4-((5-(9H-carbazol-9-yl)pentyl)oxy)-2H-chromen-2-one (**3d**)

White solid; yield 61%; mp 140 – 142 °C; IR (KBr): 3061, 2946, 2923, 2859, 2358, 2339, 1716, 1620 cm⁻¹. ¹H NMR (600 MHz, CDCl₃) δ 8.01 (dd, *J* = 7.7, 1.0 Hz, 2H), 7.54 (dd, *J* = 7.9, 1.6 Hz, 1H), 7.47 – 7.43 (m, 1H), 7.37 (td, *J* = 7.6, 7.1, 1.2 Hz, 2H), 7.32 (d, *J* = 8.1 Hz, 2H), 7.21 (d, *J* = 8.6 Hz, 1H), 7.16 – 7.12 (m, 3H), 5.49 (s, 1H), 4.28 (t, *J* = 6.9 Hz, 2H), 3.94 (td, *J* = 6.2, 2.4 Hz, 2H), 1.95 – 1.89 (m, 2H), 1.82 – 1.78 (m, 2H), 1.51 – 1.46 (m, 2H). ¹³C NMR (151 MHz, Chloroform-*d*) δ 164.4, 161.9, 152.2, 139.2, 131.2, 124.6, 122.8, 121.7, 119.3, 117.8, 115.6, 114.5, 107.4, 89.3, 67.8, 41.6, 27.6, 27.2, 22.6. HRMS: (ESI, m/z): [M+Na]⁺ calcd for C₂₆H₂₃NO₃ 420.1570, found 420.1584.

2.3. Single crystal XRD studies

Crystals of compound **3d** was grown by slow evaporation of methanol at room temperature. Diffraction intensities for the compounds were collected at 296(2) K using a Bruker SMART APEX-II CCD area-detector with MoK α radiation (λ = 0.71073 Å). The collected data were reduced with the SAINT program^[30], and multi-scan absorption corrections were performed using the SADABS program^[31]. Structures were solved by direct methods. The compounds were refined against F^2 by full-matrix least-squares methods using the SHELXTL package^[32]. All of the non-hydrogen atoms were refined anisotropically. Hydrogen atoms were placed in

calculated positions and constrained to ride on their parent atoms. The Mercury programs[33] were used to describe the molecular structures.

2.4. Hirshfeld surfaces analysis

Analysis of Hirshfeld surfaces and their associated two dimensional fingerprint plots of compound **3d** were calculated by using CrystalExplorer17[34]. The Hirshfeld surfaces are mapped with different properties d_{norm} , shape index, curvedness. The d_{norm} is normalized contact distance, defined in terms of d_e , d_i and the vdW radii of the atoms. The combination of d_e and d_i in the form of a 2D fingerprint plot displays summary of intermolecular contacts in the crystal.

2.5. In vitro ChE activity assay

The ChE inhibitory activities of test compounds **3a** – **3d** were measured using Ellman's colorimetric method with a slight modification[35]. The Ellman's assays were performed in 96 well microplate using *eeAChE*, *hAChE*, *eqBuChE*, *hBuChE*. An AChE and BuChE was dissolved in 0.1 M phosphate-buffered saline (PBS, pH 8.0) to obtain a solution of 0.35 U/mL. The compounds were dissolved in methanol and diluted with the 0.1 M phosphate-buffered saline (PBS, pH 8.0) to yield corresponding test concentrations (methanol less than 5%). In assays, 20 μL of AChE or BuChE were incubated with 10 μL of tested compounds and 130 μL of 0.1 M PBS (pH 8.0) for 10 min in 96-well microplates before addition of 20 μL of 3.33 mM DTNB solution and 20 μL of 5.30 mM ATCI (or BTCl) solution. After the addition of DTNB and ATCI (or BTCl), the 96-well microplates were read at 412 nm with a microplate reader (SPECTRAFLUOR, TECAN, Sunrise, Austria) for 15 min. One triplicate sample without inhibitors was always present to yield 100% of AChE or BuChE activity. The reaction rates were compared and the percent inhibition due to the presence of tested compounds was calculated. Tacrine was used as a positive control. All samples were assayed in triplicate.

2.6. Molecular Modeling Evaluations

The pdb structure of AChE (PDB ID: 2CMF) was obtained from the RCSB Protein Data Bank (www.rcsb.org/pdb). Docking simulations were performed on the compound **3a** - **3d** with Molecular Operating Environment (MOE)[36] using the

CHARMm force field. Enzyme structure of 2CMF was checked for missing atoms, bonds and contacts. Hydrogens and partial charges were added using the protonate 3D application in MOE. The compound **3a** - **3d** was drawn in MOE then protonated using the protonate 3D protocol and energy was minimized using the MMFF94x force field in MOE. After the enzyme and the ligand were ready for the docking study, compound **3a** - **3d** was docked into the active site of the protein by the “Triangle Matcher” method. The Dock scoring in MOE software was done using ASE scoring function and forcefield was selected as the refinement method. The best 10 poses of molecules were retained and scored. After docking, the geometry of resulting complex was studied using the MOE's pose viewer utility.

2.7. Antioxidant activity assay

The antioxidant potency was evaluated by the oxygen radical absorbance capacity-fluorescein (ORAC-FL) assay[37]. Fluorescein (FL), 6-hydroxy-2,5,7,8-tetramethylchromane-2-carboxylic acid (Trolox) and 2,2'-Azobis (amidinopropane) dihydrochloride (AAPH) was purchased from Aladdin Industrial Corporation. All the assays were performed with 75 mM phosphate buffer (pH = 7.40), and the final reaction mixture was 200 μ L. FL (120 μ L, 150 nM final concentration) and antioxidant (20 μ L) were added in the wells of a black 96-well plate using Trolox as a standard (1–8 μ M, final concentration). The plate was incubated for 20 min at 37 °C and AAPH solution (60 μ L, 12 mM final concentration) was added rapidly. Then the plate was placed in a microplate reader (SPECTRAFLUOR, TECAN, Sunrise, Austria) and the fluorescence recorded every minute for 90 min with excitation at 485 nm and emission at 535 nm. The plate was automatically shaken prior to each reading. A blank (FL + AAPH) using phosphate buffer instead of antioxidant and Trolox calibration were carried out in each assay. The samples were measured at different concentrations (1–10 μ M). All the reaction mixture was prepared in duplicate, and at least three independent assays were performed for each sample. Antioxidant curves (fluorescence versus time) were normalized to the curve of the blank in the same assay, and then the area under the fluorescence decay curve (AUC) was calculated. The net AUC of a sample was obtained by subtracting the

AUC of the blank. ORAC-FL values were expressed as Trolox equivalents by using the standard curve calculated for each sample, where the ORAC-FL value of Trolox was taken as 1, indicating the antioxidant potency of the tested compounds.

3. Result and discussion

3.1. Spectral characterization

The route for the synthesis of the desired compounds **3a-d** is illustrated in **Scheme 1**. Carbazole dimers in the first steps of the synthesis were observed. To increase the yields of the compound **2a** and **2b** and decrease the yields of dimers excessive α,ω - dibromoalkanes were used. The yields of the compound **2a** and **2b** were 56% and 60% respectively. All crude products **3a-3d** were purified by silica gel column chromatography. Purity of the obtained compounds was checked by the TLC. The compounds were characterized by FT-IR, NMR, HRMS techniques and X-ray crystallography. All the result substantiates the structures proposed.

The FT-IR spectrum of the prepared compounds are showed by a strong broad absorption at the range of 1608-1626 cm^{-1} which can be assigned to the ν (C=O) stretches. The absorption bands falling in the range of 2859-2946 cm^{-1} are corresponding to the ν (C-H) of the alkane chain for compounds **3a**, **3b**, **3c** and **3d**. The mode of ν (C-H) appears at the range of 3059-3094 cm^{-1} suggests the presence of the aromatic benzene rings of the three compounds. In the ^1H NMR spectrum of the prepared compounds, displayed the proton of the lactone ring of the coumarin ring at 6.14 ppm, 6.12 ppm, 5.46 ppm and 5.49 ppm respectively for compound **3a**, **3b**, **3c** and **3d**, and that proton is coupled with a methyl group on the lactone ring and split into a doublet respectively for compound **3a** and **3b**. And for **3c** and **3d**, that proton is a single peak. The appeared signals of all the protons of the compound **3a-3d** were found as to be in their expected region. In the ^{13}C NMR spectra the characteristic phenyl signals are observed at 107.4 ppm to 165.1 ppm for compounds **3a**, **3b**, **3c** and **3d**. The signals of the carbonyl are found at 161.6 ppm, 161.9 ppm, 165.1 ppm and 164.4 ppm for compounds **3a**, **3b**, **3c** and **3d** respectively. The carbons of alkyl chains are observed at 18.6 ppm to 68.1 ppm for the four compounds. The HRMS spectrum of compound **3a-3d** show $[\text{M}+\text{H}]^+$ peak at m/z : 384.1593, 412.1902, 370.1439 and

398.1755 corresponding to $C_{25}H_{21}NO_3 [M+H]^+$, $C_{27}H_{25}NO_3 [M+H]^+$, $C_{24}H_{19}NO_3 [M+H]^+$ and $C_{26}H_{23}NO_3 [M+H]^+$ for compound **3a**, **3b**, **3c** and **3d** respectively.

3.2. Crystal structure of the compound **3d**

The structure of compounds **3d** was demonstrated by X-ray diffraction analysis. The crystal data was presented in **Table 1**, **Figure 1** and **Figure 2** has been deposited at the Cambridge Crystallographic Data Centre as supplementary publication no. CCDC 1961036. The compound **3d** had the crystal system of monoclinic and the space group of $P2_1/c$. The selected bond lengths and angles of the compound were listed in **Table 2**. The bond lengths of O(3)-C(3) and O(3)-C(10) were 1.3413(19) Å and 1.4373(19) Å respectively. The bond length of N(1)-C(14) for compound **3d** was 1.457(2) Å. The packing diagram of the compound **3d** viewed along the axis is showed in **Figure 2**. The crystal packing diagrams of the compound showed that there is no hydrogen bond for the compound.

Table 1. Crystallographic data for the compound **3d**.

Compound	3d
Formula	$C_{26}H_{23}NO_3$
FW	397.45
Crystal shape/colour	plate/colourless
Crystal size (mm)	0.24×0.22× 0.12
<i>T</i> (K)	296(2)
λ (MoK α) (Å)	0.71073
Crystal system	monoclinic
Space group	$P2_1/c$
<i>a</i> (Å)	9.174(3)
<i>b</i> (Å)	23.827(7)
<i>c</i> (Å)	9.558(3)
α (°)	90
β (°)	101.444(5)
γ (°)	90

V (\AA^3)	2047.8(11)
Z	4
μ (MoK α) (mm^{-1})	0.084
T_{min}	0.9521
T_{max}	0.9622
D_c (g cm^{-3})	1.289
Measured reflections	12325
Unique reflections and R_{int}	4661 and 0.0417
Observed reflections	1740
data/restraints/parameters	4661/0/271
Goodness of fit on F^2	0.966
R_1 [$I \geq 2\sigma(I)$]	0.0462
wR_2 [$I \geq 2\sigma(I)$]	0.0983
R_1 (all data)	0.1037
wR_2 (all data)	0.1195
Large diff. peak and hole (e \AA^{-3})	0.13/-0.18

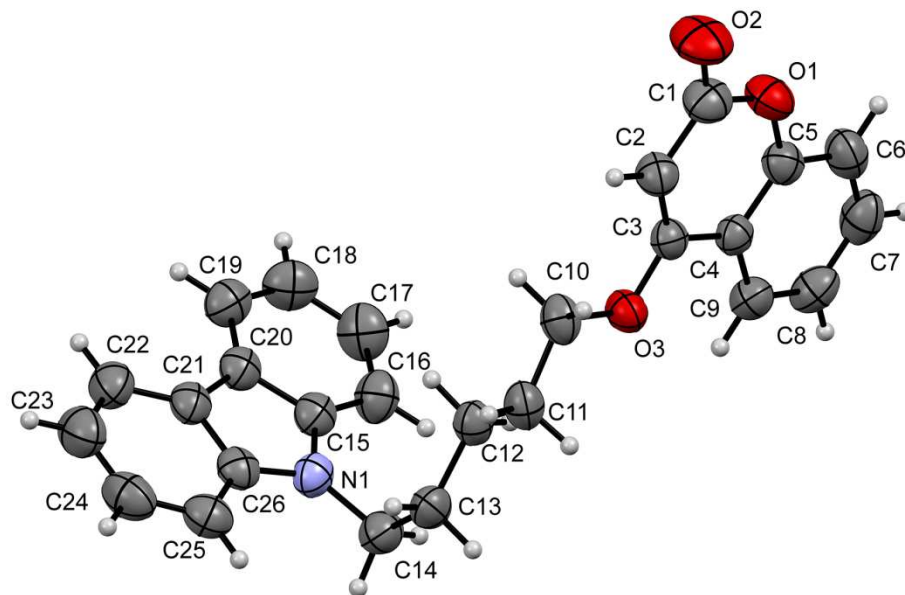


Figure 1. ORTEP of the compound **3d** with thermal ellipsoids drawn at 50% probability.

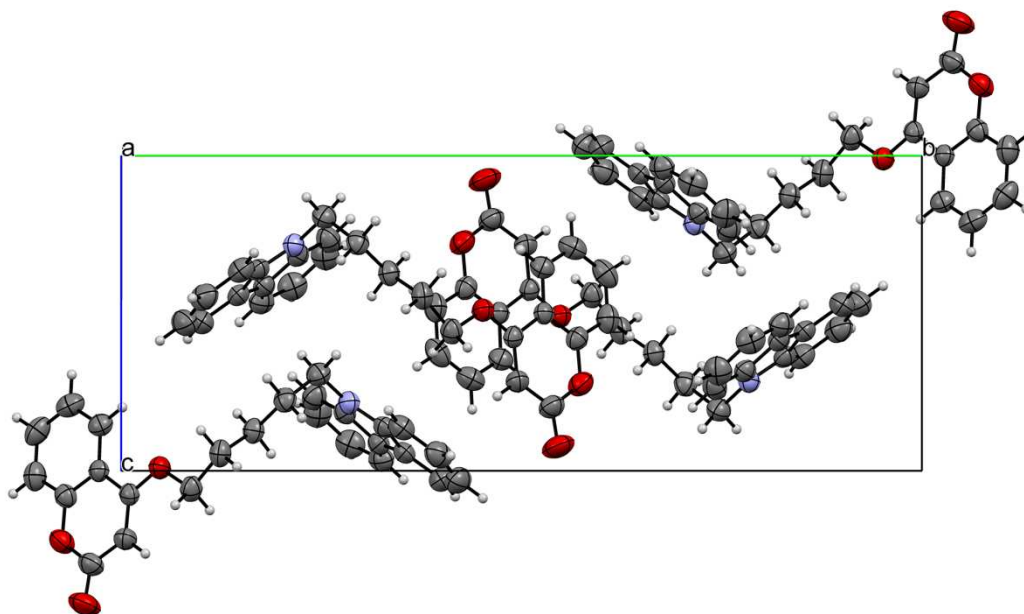


Figure 2. Packing diagrams of the compound **3d** viewed along the axis.

Table 2. Selected bond lengths (Å) and angles (°) for the compound **3d**.

Bond lengths			
O(1)-C(1)	1.380(2)	O(3)-C(10)	1.4373(19)
O(1)-C(5)	1.374(2)	N(1)-C(14)	1.457(2)
O(2)-C(1)	1.207(2)	N(1)-C(15)	1.389(2)
O(3)-C(3)	1.3413(19)	N(1)-C(26)	1.382(2)
Bond angles			
C(1)-O(1)-C(5)	121.47(14)	C(2)-C(3)-O(3)	125.74(16)
O(1)-C(1)-O(2)	116.26(18)	C(14)-N(1)-C(15)	125.64(15)
C(2)-C(1)-O(2)	126.1(2)	C(14)-N(1)-C(26)	125.81(15)
C(3)-O(3)-C(10)	117.08(13)	C(15)-N(1)-C(26)	108.42(14)

3.3. Hirshfeld surface analysis

Hirshfeld surfaces and finger print plots were generated for the compound **3d** to understand the different intermolecular interactions and packing modes. The d_{norm} mapped on Hirshfeld surface and selected 2D finger print plots of different interaction of the compound are shown in **Figure 3** and **Figure 4**. For the compound **3d**, the red regions mainly indicate C \cdots H and O \cdots H interactions. The d_{norm} map of compound shows four pairs of adjacent deep-red regions which demonstrate the C-H \cdots O and

C-H...C intermolecular interactions forming corresponding crystal packing pattern. One pairs of the deep-red regions demonstrate the strong C-H...O intermolecular interactions between the carbonyl of the coumarin part and the carbazole part of another molecule. One pairs of the deep-red regions demonstrate the strong C-H...O intermolecular interactions between the carbonyl of the coumarin part and the coumarin part of another molecule. The other two pairs of the deep-red regions demonstrate the C-H...C intermolecular interactions of the carbazole part with the carbazole part and the linker respectively.

The 2D fingerprint plots of the main intermolecular contacts for compound **3d** are showed in **Figure 4**. H...H intermolecular contact with contribution of 47.7% of the overall contacts for the compound is the major contributor to the Hirshfeld surface. The C...H intermolecular contact being one of the strong contacts with contribution of 32.0% due to the presence of C-H...C intermolecular interactions. The O...H intermolecular contact is another strong contact for compound **3d** with the contribution of 15.0% due to the presence of C-H...O intermolecular interactions. Besides the contacts mentioned above, the presence of C...C, N...H, C...O and other interactions are summarized in **Table 3**.

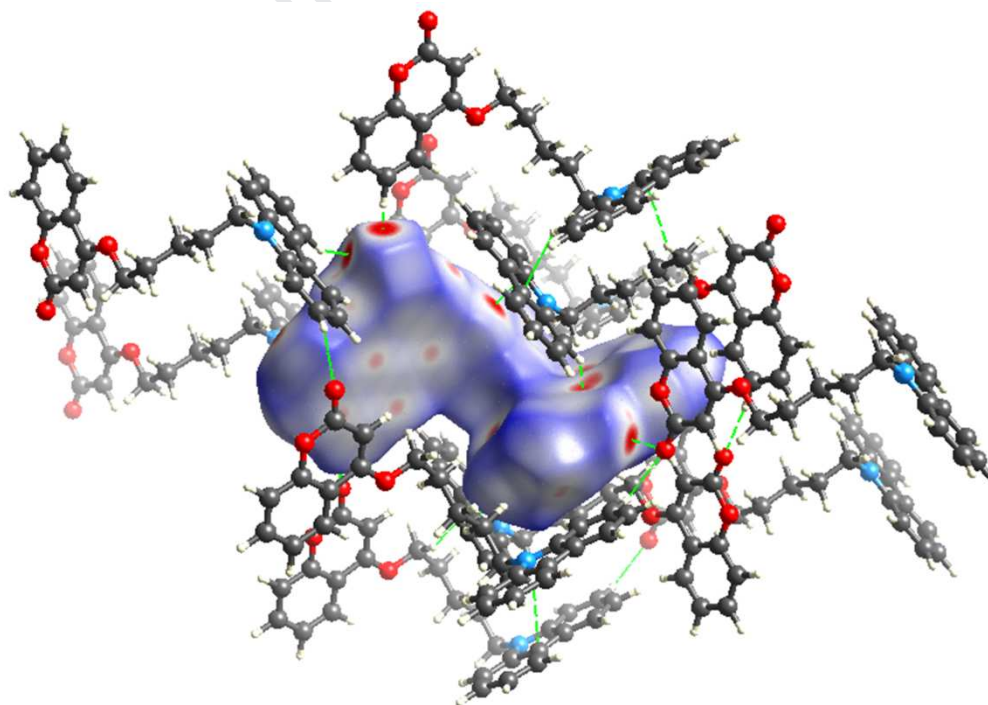


Figure 3 Hirshfeld surface mapped with d_{norm} for the compound **3d**.

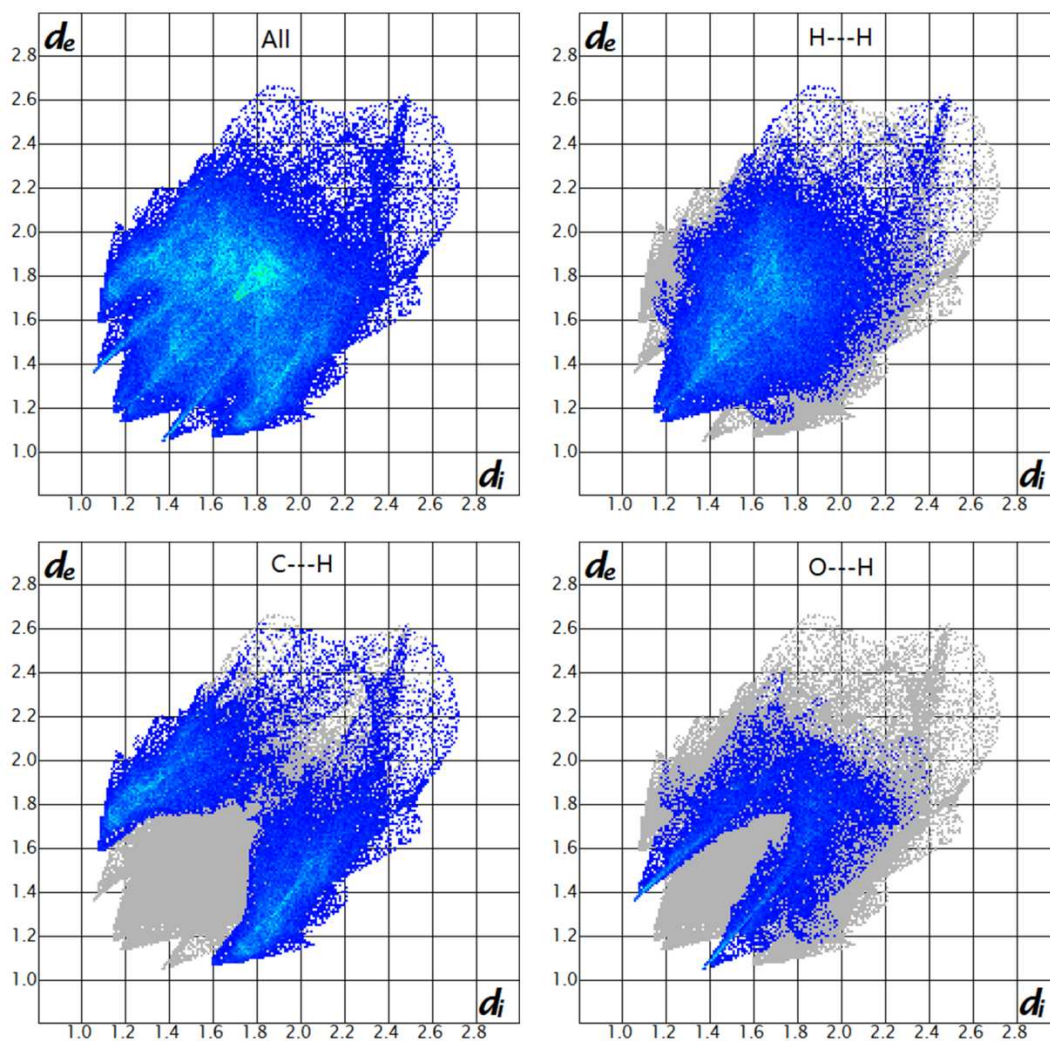


Figure 4. The 2D fingerprint plots of the compounds **3d**.

Table 3.

The percentages of the various interactions contributions to the total Hirshfeld surface area of the compound **3d**.

Interactions	Percentage (%)
H \cdots H	47.7
C \cdots H	32.0
O \cdots H	15.0
N \cdots H	0.9
C \cdots C	3.2
C \cdots O	0.8
C \cdots N	0.0

O··N	0.0
O··O	0.5
N··N	0.0

3.4 In vitro inhibition of ChEs

The inhibitory activities against ChEs were determined according to Ellman's method using tacrine as reference compounds[35]. The obtained IC₅₀ values (in μM) were presented in **Table 4**. Four of the compounds showed the *ee*AChE-inhibition activities and could inhibit the *ee*AChE dose dependently (**Figure 5**). Compound **3d** with IC₅₀ of 3.75 μM showed the best activity against *ee*AChE. While the *h*AChE inhibitory activities of the four compounds were weak. Only compound **3b** and **3d** could inhibited *h*AChE more than 30% at the concentration of 50 μM with the IC₅₀ of 76.63 μM and 70.51 μM respectively (**Figure 6**). Compound **3d** showed potent *ee*AChE inhibitory activity which was 18.8-fold more efficient for inhibition of *h*AChE. It is reported that most ChEIs exhibit the inhibitory activity for *h*ChEs in the same range as that for animal ChEs. While the inhibitory activities on *h*ChEs and animal ChEs of some compounds are very different[2, 18, 38]. None of the four could inhibit *eq*BuChE or *h*BuChE more than 30% at the concentration of 50 μM . So, compound **3b** and **3d** showed high selectivity for AChE over BuChE. These compounds would result in lesser degree of associated side effects and might be more beneficial for AD treatment because that BuChE was mainly localized in the peripheral tissues and very small amount was present in the brain region[39]. It can be seen that the inhibitory activities of the carbazole-coumarin hybrids on AChE is related to both the type of coumarin substituents and the length of the alkyl chain. It is reported that the linker length of hybrids connected the CAS and PAS binding moieties is critical for ChE inhibition[18, 40]. In this study, the inhibitory activities of the hybrids on AChE generally increases as the alkyl chain becomes longer. When the alkyl chain length is 5, the compounds (**3b** and **3d**) possessed better AChE inhibitory activities than that of compounds with alkyl chain length of 3 (**3a** and **3c**). The AChE inhibitory activities of hybrids with 4-hydroxycoumarin substituted product are better than that of 4-methylumbelliferone substitution. It is also reported that the compounds

with phenylpiperazine substitutions on the positions 4 of coumarin ring are better than that of the 6-substituted coumarins[41].

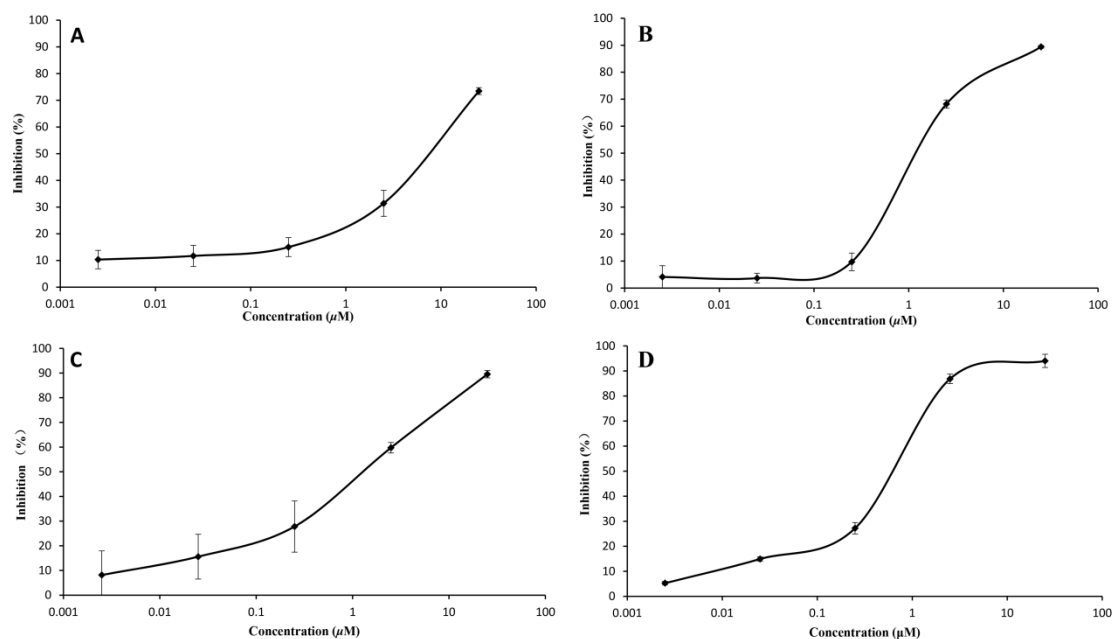


Figure 5. Dose-dependent inhibition of **3a** (A), **3b** (B), **3c** (C) and **3d** (D) against *eeAChE*. Values are means \pm SD, n=5.

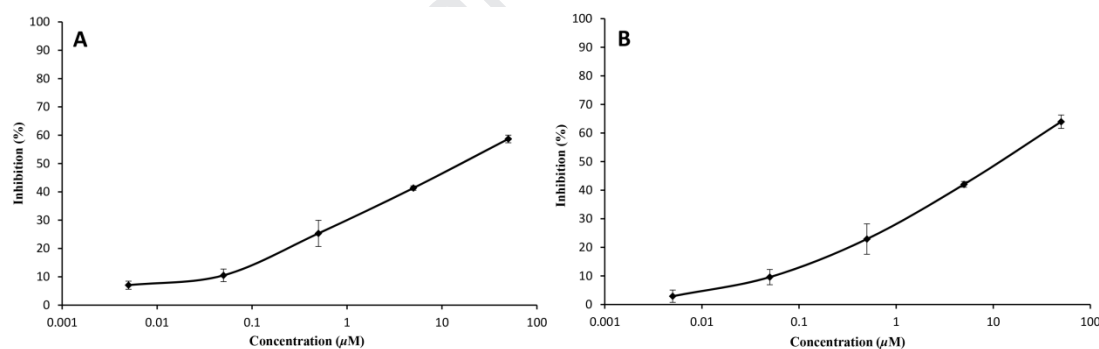


Figure 6. Dose-dependent inhibition of **3b** (A) and **3d** (B) against *hAChE*. Values are means \pm SD, n=5.

Table 4. ChEs inhibitory activities and ORAC of target compounds.

Compd.	n	IC ₅₀ (μM) ^a				ORAC ^c
		<i>eeAChE</i>	<i>eqBuChE</i>	<i>hAChE</i>	<i>hBuChE</i>	
3a	3	32.31 \pm 3.18	N/A ^b	N/A	N/A	0.96 \pm 0.018
3b	5	4.37 \pm 0.02	N/A	76.63 \pm 7.51	N/A	0.86 \pm 0.008
3c	3	5.36 \pm 0.61	N/A	N/A	N/A	0.86 \pm 0.001
3d	5	3.75 \pm 0.12	N/A	70.51 \pm 4.66	N/A	0.81 \pm 0.003

Tacrine	-	0.18±0.01	N/A	0.23±0.07	0.04±0.002	-
Trolox	-	-	-	-	-	1

^a The 50% inhibitory concentration (means ± SD of three experiments) of ChE.

^b The compound could not inhibit the ChE more than 30% at the concentration of 50 μ M.

^c Results are expressed as μ M of Trolox equivalent/ μ M of tested compounds.

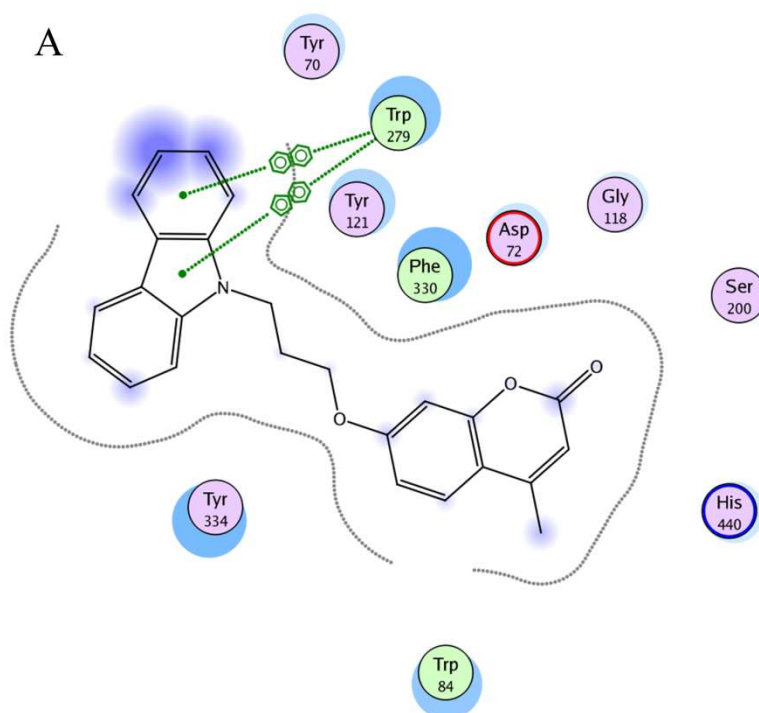
3.5 Antioxidant activity

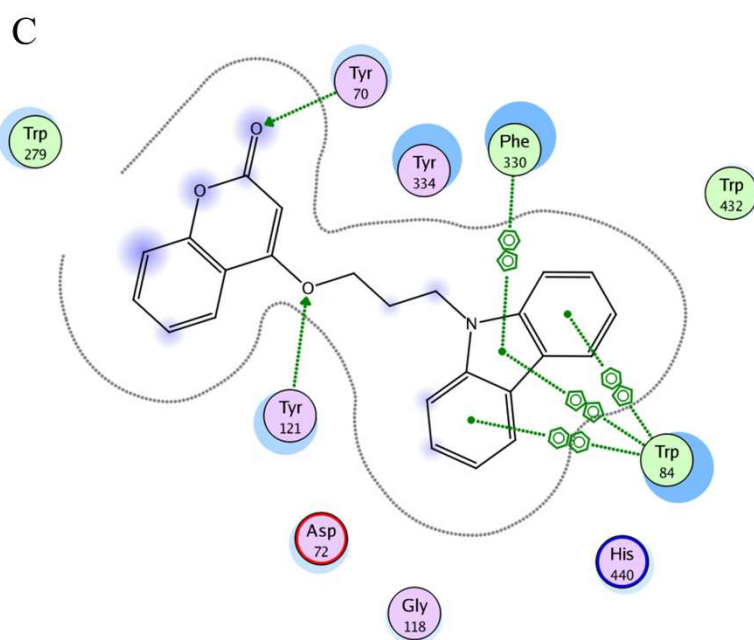
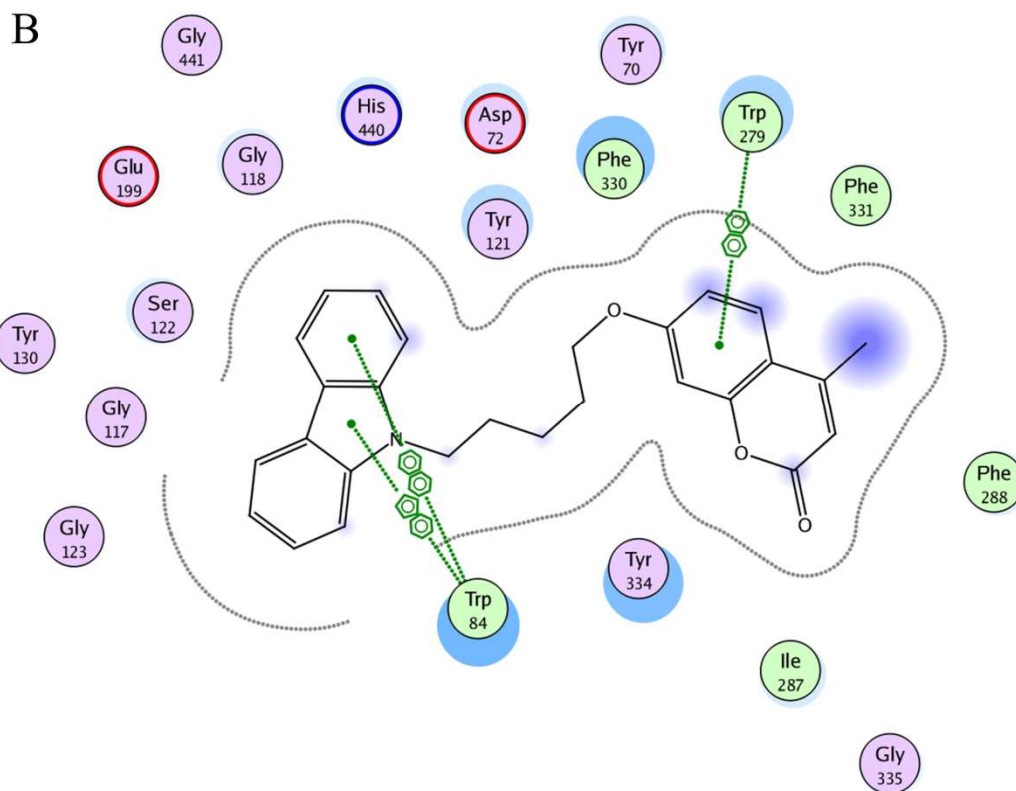
The antioxidant activities of all synthesized target compounds were determined by following the well-established ORAC-FL method (oxygen radical absorbance capacity by fluorescein) [37] and the results were shown in **Table 4**. Trolox, a vitamin E analogue, was used as the standard, and the results were expressed as Trolox equivalents. As expected, there were no oxygen radical-trapping groups in all of the compound structures, and the tested compounds did not exhibit favorable antioxidant capacity.

3.6 Molecular modeling study

To understand the binding mode of the hybrids **3a** - **3d** with the AChE, the compounds were docked with AChE (PDB code:2CMF) with MOE program. The molecule docking of the compound **3a** - **3d** with AChE showed that the compound **3b** and **3d** could interact with the CAS and the PAS of AChE as that of bis-tacrine (**Figure 7B and 7D**) with docking score of -34.80, and -34.65 kcal/mol respectively. While, compound **3a** and **3c** only interacted with the CAS of the enzyme with docking scores of -27.20 and -32.76 kcal/mol respectively (**Figure 7A and 7C**). The docking results are along with the *in vitro* AChEs-inhibition activities of the hybrids. It can be seen from the docking results that the length of the alkyl chain effected the activities of the hybrids. When the alkyl chain length is 5, the hybrids (**3b** and **3d**) could interact with both the CAS and the PAS of AChE and possessed potent AChE-inhibition activities. When the alkyl chain length is 3, the hybrids (**3a** and **3c**) only interacted with the CAS of AChE and showed weak AChE inhibitory activities. When compound **3d** which possessed the best AChE inhibitory activity was docked with AChE, the compound could interact with both the CAS and the PAS of the

enzyme like the bis-tacrine AChE (**Figure 8**, bis-tacrine was showed in green color). The carbazole part and coumarin part of the hybrids bind with CAS and PAS, respectively. The carbazole moiety was located between TRP84 and PHE330 in the PAS of the enzyme *via* the arene-arene interaction. The coumarin moiety could bind to the PAS between TRP279 and Tyr70 as reported previously[7, 42]. The carbonyl of the coumarin part could interact with TYR70 *via* the hydrogen bonds. The benzene ring of the coumarin part could interact with TRP279 *via* arene-arene interactions. It is reported that the AChEI that interacted with PAS can interfere $A\beta$ aggregation. Therefore, the hybrid **3a-3b** should be able to enhance cholinergic tone by reducing the hydrolytic activity of AChE and decreasing the deposition of $A\beta$ fibrils[28].





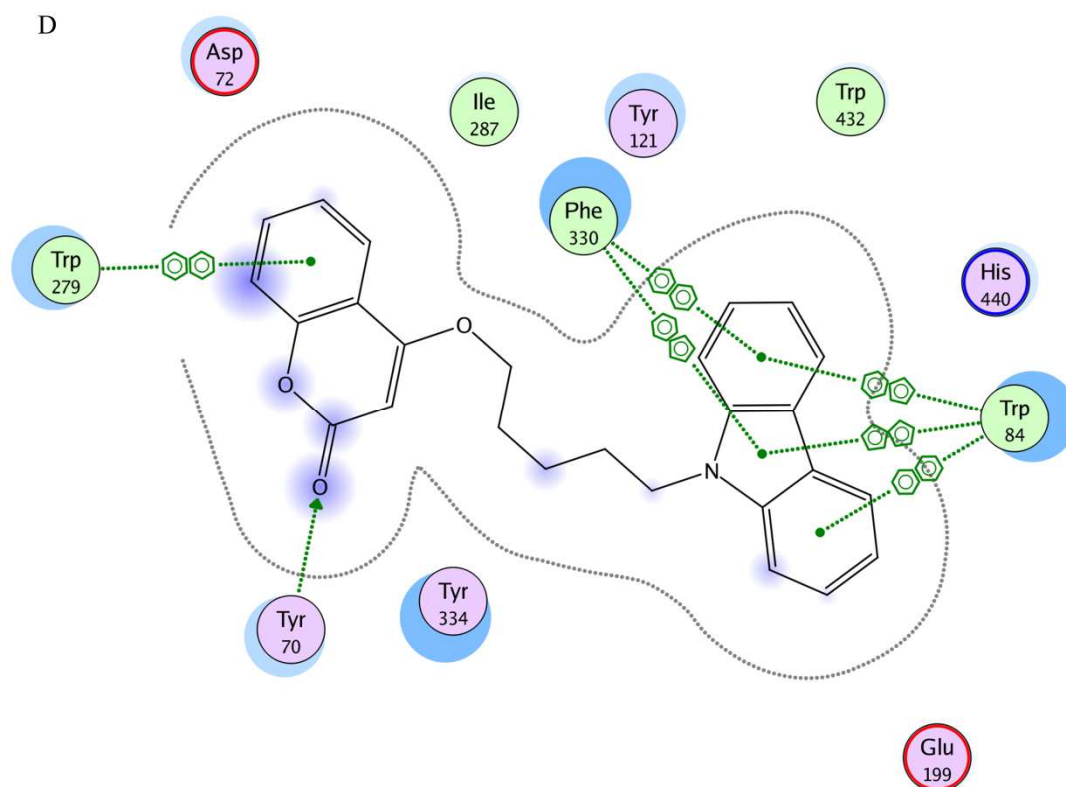


Figure 7. The AChE interaction map displaying the binding and interactions of compound of **3a** (A), **3b** (B), **3c** (C) and **3d** (D) with AChE (PDB ID 2CMF).

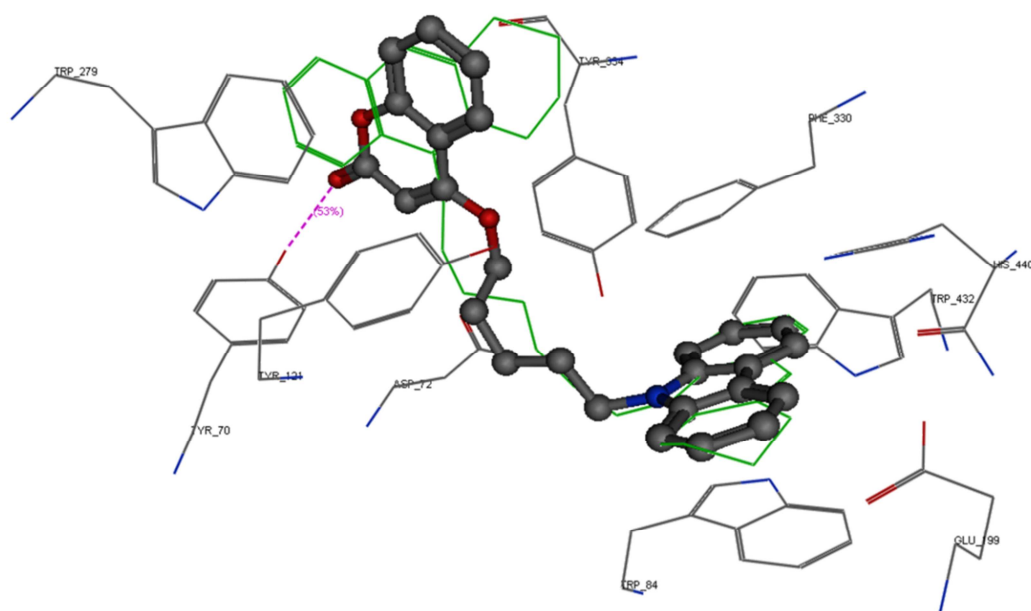


Figure 8. Close-up depiction of the docking pose of compound **3d** showing different types of ligand-enzyme interactions in the binding site of 2CMF (Bis-tacrine was showed in green color).

4. Conclusion

Four carbazole-coumarin hybrids were synthesized with simple ways and high yields. The structures of the four compounds were determined by IR, NMR, HRMS and X-ray Crystallography. The ChE inhibitory activities and antioxidant activities of the carbazole-coumarin hybrids were evaluated *in vitro*. The compound **3d**, which possessed the best AChE-inhibition activity, could interact with both the CAS and the PAS of AChE, and shown antioxidant capacity. This compound could be a promising lead candidate for the treatment of AD.

Supporting Information Summary

The Supporting Information contains the spectral data for compounds.

Acknowledgements

We gratefully acknowledge financial supports of graduate research and innovation projects of Jiangsu province (KYCX18_2579), natural science foundation of Jiangsu province (BK20191470), national natural science foundation of China (81703557) and project funded by the priority academic program development of Jiangsu higher education institutions.

Reference

- [1] 2015 Alzheimer's disease facts and figures, *Alzheimer's & Dementia* 11(3) (2015) 332-384.
- [2] S.S. Xie, X. Wang, N. Jiang, W. Yu, K.D. Wang, J.S. Lan, Z.R. Li, L.Y. Kong, Multi-target tacrine-coumarin hybrids: cholinesterase and monoamine oxidase B inhibition properties against Alzheimer's disease, *Eur J Med Chem* 95 (2015) 153-65.
- [3] B. Li, R. Pai, M. Di, D. Aiello, M.H. Barnes, M.M. Butler, T.F. Tashjian, N.P. Peet, T.L. Bowlin, D.T. Moir, Coumarin-based inhibitors of *Bacillus anthracis* and *Staphylococcus aureus* replicative DNA helicase: chemical optimization, biological evaluation, and antibacterial activities, *J. Med. Chem.* 55(24) (2012) 10896-908.
- [4] J.S. Birks, R.J. Harvey, Donepezil for dementia due to Alzheimer's disease, *Cochrane*

Database of systematic reviews (6) (2018).

[5] J.T. Olin, L. Schneider, Galantamine for Alzheimer's disease, Cochrane database of systematic reviews (3) (2002).

[6] J.S. Lan, Y. Ding, Y. Liu, P. Kang, J.W. Hou, X.Y. Zhang, S.S. Xie, T. Zhang, Design, synthesis and biological evaluation of novel coumarin-N-benzyl pyridinium hybrids as multi-target agents for the treatment of Alzheimer's disease, *Eur J Med Chem* 139 (2017) 48-59.

[7] M. Alipour, M. Khoobi, A. Moradi, H. Nadri, F. Homayouni Moghadam, S. Emami, Z. Hasanpour, A. Foroumadi, A. Shafiee, Synthesis and anti-cholinesterase activity of new 7-hydroxycoumarin derivatives, *Eur J Med Chem* 82 (2014) 536-44.

[8] H. Akrami, B.F. Mirjalili, M. Khoobi, H. Nadri, A. Moradi, A. Sakhteman, S. Emami, A. Foroumadi, A. Shafiee, Indolinone-based acetylcholinesterase inhibitors: synthesis, biological activity and molecular modeling, *Eur. J. Med. Chem.* 84 (2014) 375-81.

[9] C. Wang, Z. Wu, H. Cai, S. Xu, J. Liu, J. Jiang, H. Yao, X. Wu, J. Xu, Design, synthesis, biological evaluation and docking study of 4-isochromanone hybrids bearing N-benzyl pyridinium moiety as dual binding site acetylcholinesterase inhibitors, *Bioorg. Med. Chem. Lett.* 25(22) (2015) 5212-6.

[10] M. Rosini, E. Simoni, A. Milelli, A. Minarini, C. Melchiorre, Oxidative stress in Alzheimer's disease: are we connecting the dots?, *J. Med. Chem.* 57(7) (2014) 2821-31.

[11] L. Wang, Y. Wang, Y. Tian, J. Shang, X. Sun, H. Chen, H. Wang, W. Tan, Design, synthesis, biological evaluation, and molecular modeling studies of chalcone-rivastigmine hybrids as cholinesterase inhibitors, *Bioorganic & Medicinal Chemistry* 25(1) (2017) 360-371.

- [12] Z. Sang, K. Wang, H. Wang, L. Yu, H. Wang, Q. Ma, M. Ye, X. Han, W. Liu, Design, synthesis and biological evaluation of phthalimide-alkylamine derivatives as balanced multifunctional cholinesterase and monoamine oxidase-B inhibitors for the treatment of Alzheimer's disease, *Bioorganic & medicinal chemistry letters* 27(22) (2017) 5053-5059.
- [13] H.L. Yang, P. Cai, Q.H. Liu, X.L. Yang, S.Q. Fang, Y.W. Tang, C. Wang, X.B. Wang, L.Y. Kong, Design, synthesis, and evaluation of salicyladimine derivatives as multitarget-directed ligands against Alzheimer's disease, *Bioorg Med Chem* 25(21) (2017) 5917-5928.
- [14] H. Singh, J.V. Singh, K. Bhagat, H.K. Gulati, M. Sanduja, N. Kumar, N. Kinarivala, S. Sharma, Rational approaches, design strategies, structure activity relationship and mechanistic insights for therapeutic coumarin hybrids, *Bioorg Med Chem* 27(16) (2019) 3477-3510.
- [15] S.K. Yusufzai, M.S. Khan, O. Sulaiman, H. Osman, D.N. Lamjin, Molecular docking studies of coumarin hybrids as potential acetylcholinesterase, butyrylcholinesterase, monoamine oxidase A/B and beta-amyloid inhibitors for Alzheimer's disease, *Chem Cent J* 12(1) (2018) 128.
- [16] L.G. de Souza, M.N. Renna, J.D. Figueroa-Villar, Coumarins as cholinesterase inhibitors: A review, *Chem Biol Interact* 254 (2016) 11-23.
- [17] S. Hamulakova, L. Janovec, M. Hrabínova, K. Spilovska, J. Korabecny, P. Kristian, K. Kuca, J. Imrich, Synthesis and biological evaluation of novel tacrine derivatives and tacrine-coumarin hybrids as cholinesterase inhibitors, *J Med Chem* 57(16) (2014) 7073-84.
- [18] S.S. Xie, J.S. Lan, X. Wang, Z.M. Wang, N. Jiang, F. Li, J.J. Wu, J. Wang, L.Y. Kong, Design, synthesis and biological evaluation of novel donepezil-coumarin hybrids as

multi-target agents for the treatment of Alzheimer's disease, *Bioorg Med Chem* 24(7) (2016) 1528-39.

[19] A. Hiremathad, K. Chand, R.S. Keri, Development of coumarin-benzofuran hybrids as versatile multitargeted compounds for the treatment of Alzheimer's Disease, *Chem Biol Drug Des* 92(2) (2018) 1497-1503.

[20] Q. Sun, D.Y. Peng, S.G. Yang, X.L. Zhu, W.C. Yang, G.F. Yang, Syntheses of coumarin-tacrine hybrids as dual-site acetylcholinesterase inhibitors and their activity against butylcholinesterase, Abeta aggregation, and beta-secretase, *Bioorg Med Chem* 22(17) (2014) 4784-91.

[21] C. Zhang, K. Yang, S. Yu, J. Su, S. Yuan, J. Han, Y. Chen, J. Gu, T. Zhou, R. Bai, Design, synthesis and biological evaluation of hydroxypyridinone-coumarin hybrids as multimodal monoamine oxidase B inhibitors and iron chelates against Alzheimer's disease, *Eur. J. Med. Chem.* 180 (2019) 367-382.

[22] Z. Najafi, M. Mahdavi, M. Saeedi, E. Karimpour-Razkenari, N. Edraki, M. Sharifzadeh, M. Khanavi, T. Akbarzadeh, Novel tacrine-coumarin hybrids linked to 1, 2, 3-triazole as anti-Alzheimer's compounds: In vitro and in vivo biological evaluation and docking study, *Bioorg. Chem.* 83 (2019) 303-316.

[23] S. Thiratmatrakul, C. Yenjai, P. Waiwut, O. Vajragupta, P. Reubroycharoen, M. Tohda, C. Boonyarat, Synthesis, biological evaluation and molecular modeling study of novel tacrine-carbazole hybrids as potential multifunctional agents for the treatment of Alzheimer's disease, *Eur. J. Med. Chem.* 75 (2014) 21-30.

[24] Y.-Z. Tang, Z.-Q. Liu, Free-radical-scavenging effect of carbazole derivatives on

- AAPH-induced hemolysis of human erythrocytes, *Biorg. Med. Chem.* 15(5) (2007) 1903-1913.
- [25] W. Yang, Y. Wong, O.T. Ng, L.P. Bai, D.W. Kwong, Y. Ke, Z.H. Jiang, H.W. Li, K.K. Yung, M.S. Wong, Inhibition of Beta-Amyloid Peptide Aggregation by Multifunctional Carbazole-Based Fluorophores, *Angew. Chem. Int. Ed.* 51(8) (2012) 1804-1810.
- [26] L. Fang, X. Fang, S. Gou, A. Lupp, I. Lenhardt, Y. Sun, Z. Huang, Y. Chen, Y. Zhang, C. Fleck, Design, synthesis and biological evaluation of D-ring opened galantamine analogs as multifunctional anti-Alzheimer agents, *Eur J Med Chem* 76 (2014) 376-86.
- [27] L. Fang, M. Chen, Z. Liu, X. Fang, S. Gou, L. Chen, Ferulic acid-carbazole hybrid compounds: Combination of cholinesterase inhibition, antioxidant and neuroprotection as multifunctional anti-Alzheimer agents, *Bioorg Med Chem* 24(4) (2016) 886-93.
- [28] S. Thiratmatrakul, C. Yenjai, P. Waiwut, O. Vajragupta, P. Reubroycharoen, M. Tohda, C. Boonyarat, Synthesis, biological evaluation and molecular modeling study of novel tacrine-carbazole hybrids as potential multifunctional agents for the treatment of Alzheimer's disease, *Eur J Med Chem* 75 (2014) 21-30.
- [29] G.F. Makhaeva, E.F. Shevtsova, N.P. Boltneva, S.V. Lushchekina, N.V. Kovaleva, E.V. Rudakova, S.O. Bachurin, R.J. Richardson, Overview of novel multifunctional agents based on conjugates of gamma-carbolines, carbazoles, tetrahydrocarbazoles, phenothiazines, and aminoadamantanes for treatment of Alzheimer's disease, *Chem Biol Interact* 308 (2019) 224-234.
- [30] Bruker, SMART (Version 5.628) and SAINT (Version 6.02); Bruker AXS Inc: Madison, WI (1998).
- [31] G.M. Sheldrick, SADABS. Program for Empirical Absorption Correction of Area Detector;

University of Göttingen: Göttingen, Germany (1996).

[32] G.M. Sheldrick, SHELXTL V5.1. Software Reference Manual; Bruker AXS: Madison, WI (1997).

[33] C.F. Macrae, I.J. Bruno, J.A. Chisholm, P.R. Edgington, P. McCabe, E. Pidcock, L. Rodriguez-Monge, R. Taylor, J. van de Streek, P.A. Wood, Mercury CSD 2.0 - new features for the visualization and investigation of crystal structures, *Journal of Applied Crystallography* 41(2) (2008) 466-470.

[34] J.J.M. M.J. Turner, S.K. Wolff, D.J. Grimwood, P.R. Spackman, D. Jayatilaka, M.A. Spackman, *CrystalExplorer 17*, University of Western Australia 2017 (2017).

[35] G.L. Ellman, K.D. Courtney, V. Andres Jr, R.M. Featherstone, A new and rapid colorimetric determination of acetylcholinesterase activity, *Biochem. Pharmacol.* 7(2) (1961) 88-95.

[36] Molecular Operating Environment (MOE), Version 2015.10.

[37] Y. Li, X. Qiang, L. Luo, X. Yang, G. Xiao, Q. Liu, J. Ai, Z. Tan, Y. Deng, Aurone Mannich base derivatives as promising multifunctional agents with acetylcholinesterase inhibition, anti-beta-amyloid aggregation and neuroprotective properties for the treatment of Alzheimer's disease, *Eur. J. Med. Chem.* 126 (2017) 762-775.

[38] Q. He, J. Liu, J.S. Lan, J. Ding, Y. Sun, Y. Fang, N. Jiang, Z. Yang, L. Sun, Y. Jin, S.S. Xie, Coumarin-dithiocarbamate hybrids as novel multitarget AChE and MAO-B inhibitors against Alzheimer's disease: Design, synthesis and biological evaluation, *Bioorg Chem* 81 (2018) 512-528.

[39] N. Jiang, Q. Huang, J. Liu, N. Liang, Q. Li, Q. Li, S.S. Xie, Design, synthesis and biological

evaluation of new coumarin-dithiocarbamate hybrids as multifunctional agents for the treatment of Alzheimer's disease, *Eur J Med Chem* 146 (2018) 287-298.

[40] S.S. Xie, J.S. Lan, X.B. Wang, N. Jiang, G. Dong, Z.R. Li, K.D. Wang, P.P. Guo, L.Y. Kong, Multifunctional tacrine-trolox hybrids for the treatment of Alzheimer's disease with cholinergic, antioxidant, neuroprotective and hepatoprotective properties, *Eur J Med Chem* 93 (2015) 42-50.

[41] X. Zhou, X.B. Wang, T. Wang, L.Y. Kong, Design, synthesis, and acetylcholinesterase inhibitory activity of novel coumarin analogues, *Bioorg Med Chem* 16(17) (2008) 8011-21.

[42] A. Asadipour, M. Alipour, M. Jafari, M. Khoobi, S. Emami, H. Nadri, A. Sakhteman, A. Moradi, V. Sheibani, F. Homayouni Moghadam, A. Shafiee, A. Foroumadi, Novel coumarin-3-carboxamides bearing N-benzylpiperidine moiety as potent acetylcholinesterase inhibitors, *Eur J Med Chem* 70 (2013) 623-30.

- Synthesis and X-ray crystallographic analysis of carbazole-coumarin hybrids.
- Experimental spectroscopic analysis (FT-IR, ^1H NMR and ^{13}C NMR) of synthesized carbazole-coumarin hybrids.
- Enzyme inhibition and antioxidant study of synthesized carbazole-coumarin hybrids.
- Molecular docking and Hirshfeld surface analysis.

Journal Pre-proof

Declaration of interests

The authors declare that they have no known competing financial interests or personal relationships that could have appeared to influence the work reported in this paper.

The authors declare the following financial interests/personal relationships which may be considered as potential competing interests:

Journal Pre-proof